(Reprinted from Nature New Biology, Vol. 229, No. 7, pp. 197–201, February 17, 1971)

Lipid and Protein Arrangement in Bacteriophage PM2

S. C. HARRISON & D. L. D. CASPAR
Laboratory of Structural Molecular Biology, Children's Cancer Research Foundation, Boston, Massachusetts 02115
R. D. CAMERINI-OTERO & R. M. FRANKLIN
Public Health Research Institute of the City of New York, New York 10016

X-ray structure analysis shows that the lipid of bacteriophage PM2 is organized in a bilayer. These results provide a basis for interpreting electron micrographs of the virus in molecular terms.

THE marine bacteriophage, PM2, is a lipid-containing virus particle[1–3], which is readily obtained in quantities sufficient for physico-chemical analysis. Our X-ray structure analysis has revealed details of the distribution of lipid and protein in the particle which correlate with the images of it seen in the electron microscope. The lipid organization of PM2 is similar to the bilayers found in myelin and in various lipid and lipoprotein model systems[4–9]. The envelopes of many animal viruses also contain lipid[10–13].

The PM2 particle has a weight of about 5.8×10^7 daltons, measured by sedimentation equilibrium (R. D. Camerini-Otero and R. M. Franklin, in preparation). It contains a single, circular molecule of double stranded DNA, of molecular weight 6×10^6 (ref. 14). Table 1 shows its protein and lipid composition. Electron microscopy shows that the particle is distinctly icosahedral in shape and approximately 600 Å in diameter[3]. Images of negatively stained particles generally show a stain-excluding peripheral band; a narrow, stain penetrable region just within; and a stain excluding "core" (images labelled A in Fig. 1*a*, *b*). Small, brush-like "spikes" are sometimes evident at the icosahedral vertices. Occasionally, stain penetrates to the particle interior, leaving an unstained band about 450 Å in diameter (images labelled B in Fig. 1*a*, *b*). We have found that this band corresponds to the lipid bilayer. In thin section, positively stained particles have a "double track" pattern at their edge (Fig. 1*c*) similar to the "unit membrane" image described by Robertson[16]. Dense but irregular depositions of stain appear at the centre of the particle.

Table 1 Chemical Analysis of Bacteriophage PM2

General composition (Camerini-Otero, R. D., and Franklin, R. M., in preparation).

DNA: 10–11%; lipid: 14–16%, of which over 90% is phospholipid; protein: approx. 75%; carbohydrate: trace.

DNA[14]

42–43% guanine-cytosine.

Lipid

Phospholipid[15]

Phosphatidyl glycerol: 67%; phosphatidyl ethanolamine: 27%; others: approx. 4%.

Fatty acids (Camerini-Otero, R. D., and Franklin, R. M., in preparation).

$C_{14:0}$: 3.0%; $C_{16:0}$: 12.0%; $C_{16:1}$: 56.6%; $C_{17:0}$: 7.3%; $C_{18:1}$: 13.9%; others: approx. 7.2%.

Proteins (Datta, A., Camerini-Otero, R. D., Braunstein, S. N., and Franklin, R. M., unpublished observations)[17]

Components	Molecular weight	No. of chains particle*
I	43,000	190
II	34,000	650
III	12,500	730
IV	4,600	660

* Estimated uncertainty about 15%.

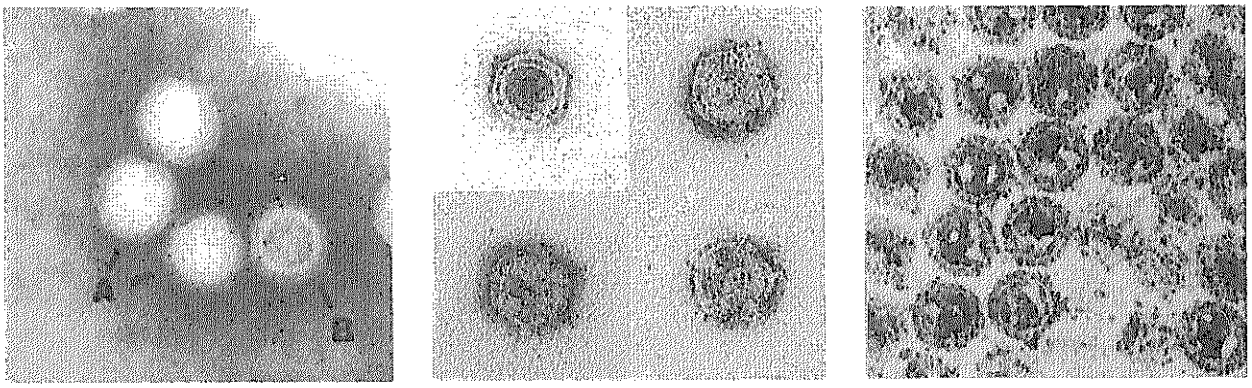

a *b* *c*

Fig. 1 Electron micrographs of PM2, ×180,000. *a*, Negatively stained with phosphotungstic acid. *b*, Negatively stained with uranyl acetate. The upper left hand particle is filled with stain, like the particle labelled B in *a*. *c*, Pelleted, embedded, sectioned and stained with uranyl acetate and lead citrate.

X-ray Pattern

Centrifuged pellets of spherical viruses generally have some local regularity of packing but no long-range ordering[17]. The recorded X-ray scattering is therefore a spherical average of the individual particle diffraction, and interparticle interference effects are restricted to the very low resolution part of the pattern. X-ray photographs from such concentrated specimens of PM2 are shown in Figs. 2*a* and *b*. The first, taken with a long specimen-to-film distance, shows the small-angle region; the second, taken with a short specimen-to-film distance, shows the diffraction out to wider angles.

The series of regularly spaced fringes in the small-angle pattern (Fig. 2*a*) is similar to the images of many cell membranes seen by electron microscopy[18]. This part of the pattern can be used to calculate the spherically averaged electron density[19–22]. The sharpness of the rings indicates that the individual particles are isometric and identical: irregularity in shape or inhomogeneity in size would smear out the diffraction fringes.

The wider-angle pattern (Fig. 2*b*) is less detailed, but contains several interesting reflexions. The relatively sharp rings, observed at 13.7, 12.0 and 10.4 Å, indicate macromolecular order that cannot yet be attributed to a particular part of the structure. The diffuse scatter in the 10 Å region is characteristic of protein. The 3.4 Å ring corresponds to the strong meridional reflexion from the B form of DNA[21]. The broad maximum at 4.5 to 4.6 Å is characteristic of liquid paraffins and of lipid phases with liquid-like packing of hydrocarbon chains[22].

A limiting resolution for computing the radial electron density of a particle from its spherically averaged diffraction is set by the widest angle at which the spherically symmetric (zero-order) term can be distinguished from higher-order terms and from background (see refs. 19 and 22). Contributions from non-spherically symmetric features of the structure are signalled by the broad, initial maximum of the corresponding higher-order spherical Bessel function appearing some distance from the centre of the pattern. The single series of periodic fringes in the small-angle X-ray pattern from PM2 (Fig. 2*a*) indicates that spherically symmetric diffraction is significant to a spacing of about 25 Å. The zero-order term can, indeed, be followed to considerably higher resolution than has been possible with other isometric viruses[17,19,23]. The strength of the spherically symmetric component can be attributed to strong radial contrast of low density lipid hydrocarbon with high density protein, nucleic acid and lipid phosphate. To compute the radial electron density, it is necessary to take the square root of the diffracted intensity after background correction, allocate signs to the various amplitude maxima, and perform a spherical Fourier synthesis*.

We have carried out these calculations on diffraction data from PM2 in buffer containing various amounts of sucrose. The observed scattered amplitude is in each case the Fourier transform of the net particle electron density, referred to the solvent density as zero*. Incremental alteration of the solvent density with sucrose therefore produces changes in the diffraction pattern, which can be used to resolve sign ambiguities and to obtain densities on an absolute scale. Transforms of PM2 in three different solvents are shown in Fig. 3 and the corresponding Fourier synthesis in Fig. 4.

We have obtained a common scale for the three transforms in Fig. 3. The scaling is possible because we can establish that the virus particle structure is not altered by added sucrose. If addition of sucrose to the buffer results merely in a uniform increase of the electron density in solvent-accessible spaces, then the difference between transforms 1 and 2 will be proportional at all points to the difference between transforms 2 and 3. The constant of proportionality is just the ratio of the two solvent electron density increments. Calculation of scale factors for transforms 2 and 3 (relative to 1) that produce this proportionality is straightforward because about fifteen fringes are measured in each pattern. That such scale factors can be found therefore validates the assumption that structural alteration in the particle does not occur as sucrose is added and that there is no significant concentration-dependent sucrose binding or exclusion.

This conclusion implies that any volume in the PM2 particle may be divided into "solvent-excluding regions", for example, protein, DNA, lipid or bound water, and into "solvent-accessible regions"[17,24]. As sucrose is added to the solvent, its concentration in the internal solvent-accessible space increases correspondingly. We can determine, in these conditions, the absolute value of the mean electron density of solvent-excluding regions at any radius in the PM2 particle*. The results of this calculation are shown in Fig. 5*a*. Because the solvent density is known, the major sources of experimental uncertainty are the relative scale of the three sets of data and the error introduced by extrapolation of scattered intensity near zero angle. There is, however, no arbitrary element in the analysis, because we have introduced no *ad hoc* assumptions about the nature of the structure, either in the computation of the Fouriers themselves or in the absolute density calculation.

X-ray Diffraction and Electron Microscopy

The most prominent feature of the electron density curves in Fig. 4 is the deep minimum centred at $r = 220$ Å. The density profile clearly resembles a low resolution view of an isolated phospholipid bilayer[6–8]. The peaks at 200 Å and at 240 Å indicate the mean radii of lipid polar groups; their separation represents a reasonable inter-polar-group distance for an average fatty-acid chain length of 16 carbons. The absolute density of the intervening minimum is about 0.30 e/Å^3. A value this low indicates that a large fraction of the solvent-excluding space must be occupied by the hydrocarbon chains[6–8].

At radii greater than 240 Å, there is a peak about 60 Å in radial extent. The peak diminishes with increasing sucrose concentration, and the calculated particle density is about 0.41 e/Å^3. The maximum must therefore represent an external protein[24], which should constitute a relatively large fraction of the total particle weight. The subunits of this protein seem to extend from the lipid polar groups to the outer margin of the virus particle. The mean outer radius is 300 Å. The minimum seen at $r = 250$ Å in the absence of sucrose is filled in the high-sucrose Fourier. A significant fraction of the volume just outside the lipid bilayer must therefore be solvent-accessible.

Features in the electron-density profile can be correlated with images of the PM2 particle in the electron microscope. Two significant details of negative staining correspond to aspects of the structure as seen by X-ray diffraction: the stain excluding region ($r = 220$ Å), identified with the bilayer,

* The spherical Fourier transform is given by

$$g(r) = 2/r \int_0^\infty f(s) \sin(2\pi rs)\, sds$$

$f(s)$ represents the scattering amplitude, including sign, as a function of the radius, s, in reciprocal space. The function $g(r)$ is the difference between particle and solvent densities:

$$g(r) = \rho(r) - \rho_0$$

where $\rho(r)$ is the electron density at a distance, r, from the particle centre and ρ_0 is the solvent electron density.

* The electron density, $\rho_0(r)$, of any solvent-excluding region can in principle be matched by a solvent of the appropriate density. We have determined experimentally the difference, $g(r)$, between the density at any radius in the particle and the density of solvent ($g(r) = \rho(r) - \rho_0$), and we have scaled $g(r)$ in the same units for three different solvents. At any radius, r', we thus have three points on a plot of $g(r')$ as a function of ρ_0. Extrapolating to zero, we can find the value of ρ_0 that would match the mean electron density of solvent-excluding regions at r'. This value is, by definition, equal to $\rho_0(r')$. One can also obtain the volume fraction accessible to solvent at any radius, if an absolute scale for the diffracted intensity is established. See ref. 19 for a detailed argument.

and the stain-accessible region (r=250 Å), identified with the boundary between the bilayer and the external protein coat. In thin sections of positively stained particles, the position of the double-track image at the periphery matches the position of the bilayer profile in our X-ray Fourier synthesis. The radius of the unstained strip is about 220 Å, just that of the electron density minimum, and the radii and widths of the two darkly staining bands suggest that they may include not only lipid polar groups but portions of the adjacent protein as well. The packing diameter in sectioned centrifuge pellets is 600 Å^3, the same as the outside diameter deduced from the X-ray analysis.

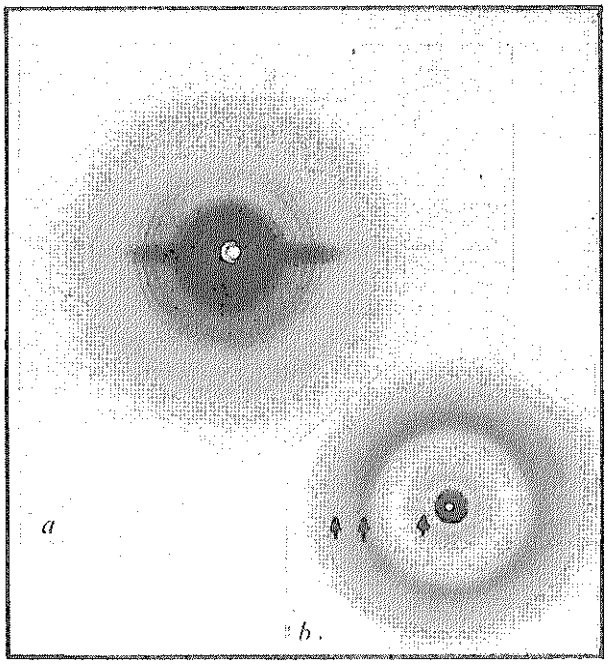

Fig. 2 *a*, Small-angle X-ray scattering photograph from PM2 in 1 M NaCl, 0.02 M Tris *p*H 7.1; 0.01 M $CaCl_2$ (NTC buffer). The virus was purified by the procedure of Silbert *et al.*[3]. The sample for X-ray scattering was prepared by centrifugation and mounted in a quartz capillary; the photograph was taken with quartz-monochromatized Cu Kα radiation from a rotating-anode, microfocus X-ray tube. The horizontal streak is parasitic scattering from the monochromator; the innermost fringes are over-exposed. Note that the outermost fringes (extending to about 25 Å) are superposed on a more diffuse "background" ring, centred at 28.5 Å. Scale: 1 cm=0.0195 Å^{-1}. *b*, Wider-angle X-ray scattering from PM2. Sample prepared as in legend for *a* and photographed on a Franks camera using Cu Kα radiation. The over-exposed disk at the centre corresponds to the entire pattern shown in *a*. Arrows indicate the sharp reflexions near 12 Å, the broad 4.6 Å band, and the 3.4 Å ring.

For a detailed examination of the electron density profile, some consideration of the shape of the PM2 particle is important. The distinctly icosahedral appearance of the phage in the electron microscope suggests that the bilayer itself may be somewhat polyhedral. If we think of the electron density as constant on nested icosahedral shells, rather than on spheres, any point in the spherically averaged electron density profile will represent a weighted average over a range of such shells. In the bilayer region, the averaging of an icosahedral structure will smear out the profile over a distance of about 15 Å, but a correction can be made by a deconvolution procedure. The results of this calculation show that if the lipid shell is indeed icosahedral in shape, the inter-polar-group distance may be about 15% smaller than the uncorrected thickness. The actual shape probably corresponds to a somewhat bloated icosahedron. The effect of the shape correction on the electron density values is harder to estimate, but any smearing out of a density profile would raise the value at a minimum and lower it at a maximum. The value of 0.30 e/Å^3 quoted above may therefore be taken as an upper limit of the actual density of solvent-excluding regions at r=220 Å.

The density at the centre of the phospholipid bilayer depends on the degree to which the terminal methyl groups of fatty-acid chains are localized near the mid-plane. The electron density of a -CH_3 is approximately 0.17 e/Å^3, compared with 0.30 e/Å^3 for -CH_2- (ref. 7). An average of one -CH_3 in six -CH_2- in the central region of the bilayer would have a density of 0.26 e/Å^3. The presence of protein in the lipid bilayer would raise this value: the mean density of protein is at least 0.40 e/Å^3 (ref. 24). We therefore conclude that the measured value of 0.30 e/Å^3 for the density at r=220 Å implies that protein occupies less than a third of the surface area at this radius.

Lipid Bilayer

The character of the electron density curve near r=220 Å indicates that the basic lipid structure in PM2 is a bilayer. If we assume, from the position of peaks assigned to polar groups, that lipid is contained between radii of 200 Å and 240 Å, the volume occupied is 2.5×10^7 Å^3. Taking an average phospholipid of molecular weight 700 and partial specific volume 1.0 cm^3/g (ref. 7), we calculate that about 2×10^4 mol of lipid per mol of virus would be required to form a complete bilayer. The measured phospholipid content of PM2 is about 1.3×10^4 mol per mol of virus. It seems from the correlation of chemical and structural results that lipid may occupy only about 65% of the area at r=220 Å. The bilayer may be fenestrated or separated into patches; in particular, we might expect special structures at the icosahedral vertices.

How does the electron density profile of the PM2 bilayer compare with results from similar lipid structures? The density maxima at radii of 200 Å and 240 Å represent the lipid polar groups, and the deep intervening minimum indicates the position of lipid hydrocarbon. Comparable structures for which measurements have been reported are nerve myelin[4,5] and lamellar L-α phase of beef-heart mitochondrial phospholipid[6]. In both cases, the mean fatty-acid chain length is about 18 carbons, compared with 16 in PM2, but the consequent difference in thickness should be not more than 10%. Blaurock[4] has computed a Fourier synthesis at 30 Å resolution for frog sciatic myelin and determined absolute electron densities by a solvent-change method similar to the one applied here. The inter-polar-group distance is 45 Å and the density at the bilayer centre is about 0.27 e/Å^3. The presence of cholesterol in myelin should produce a stiffening of the fatty-acid chains, thereby increasing the bilayer thickness[25]. The results described by Gulik-Krzywicki *et al.* for mitochondrial phospholipids[6] are in a less convenient form for comparison, because they do not show a direct Fourier synthesis. The quoted thickness for a bimolecular leaflet in the L-α phase at 25° C is 40 Å. A simple "square-well" model, with electron densities of 0.29 e/Å^2 and 0.43 e/Å^3 in the hydrocarbon and polar group regions respectively, fits the combined X-ray and mass-density measurements. These comparisons are clearly in accord with the present results from PM2.

The small radius of the PM2 bilayer suggests asymmetry in its organization. The area of a spherical shell with a radius of 200 Å (the radius of the inner polar groups) is a third smaller than the area of a 240 Å shell (outer polar groups). There will be a progressive dilution of fatty acid chains that extend outward from the inner surface of the bilayer, and a progressive concentration of chains that extend inward from its outer surface. A polyhedral form would concentrate all distortions at its edges. The bilayer could then be essentially planar and symmetric with some special structure to accomplish the necessary bends.

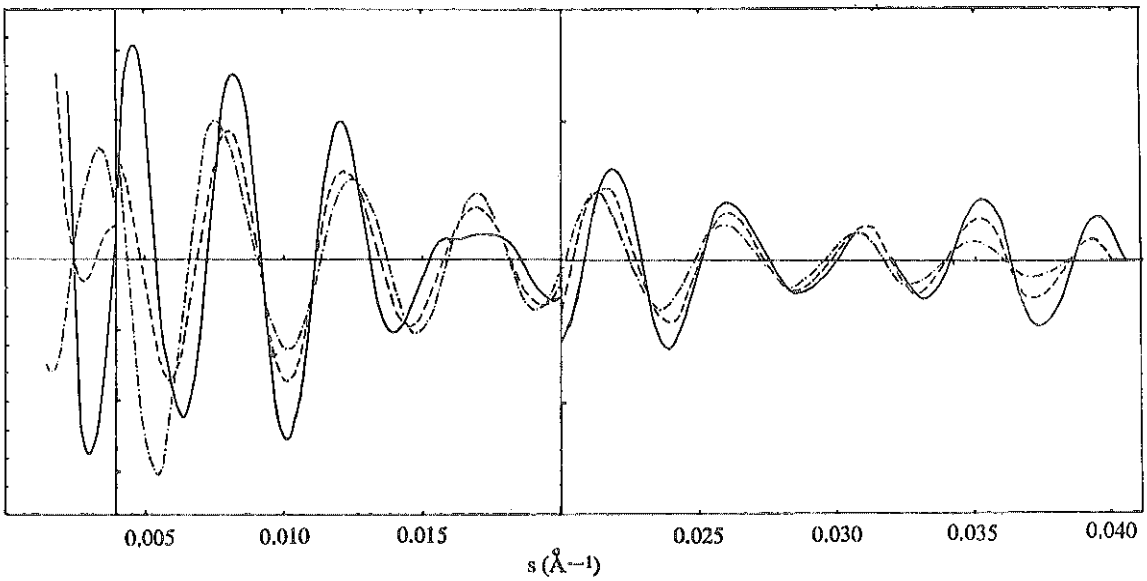

Fig. 3 The transform of PM2 in three different solvents: curve 1, NTC buffer (ρ_0=0.344 e/Å^3), ——; curve 2, NTC +30% sucrose (ρ_0=0.375 e/Å^3), - - -; curve 3, NTC+50% sucrose (ρ_0=0.394 e/Å^3), ·····. The data were obtained by photometering photographs, such as the one shown in Fig. 2*a*, on an automatic rotating-drum two-dimensional scanning microdensitometer (Optronics International) and integrating the scan around the circular fringes. The pattern of the curves near zero angle is not shown. We used the Guinier method for obtaining the zero-angle extrapolation of curve 1[18]. For curve 3, the solvent electron density (ρ_0=0.394 e/Å^3) matches the mean density of the particle, calculated from its buoyant density (1.24 g cm^{-3}) in sucrose solution; the scattered intensity at zero angle should therefore be zero. The curves shown represent the square roots of the measured intensity distributions, plotted as a function of $s=2\sin\theta/\lambda$. In the case of curves 2 and 3, the signs of successive fringes must alternate (by the principle of minimum wavelength)[34]. Signs for 1 were chosen consistent with the assumption of a uniform change in the transforms as the solvent density increases. The vertical scale (arbitrary units) changes at s=0.004 Å^{-1} and again at s=0.020 Å^{-1}; the small divisions on the ordinate lines at these points indicate identical amplitude increments.

Proteins of PM2

The form of the PM2 particle must be determined by the assembly properties of one or more of its proteins, because lipid-lipid interactions could not define so regular a structure. There is evidence for at least three structurally distinct locations that must be occupied by protein: (1) an external surface protein, indicated by the broad outer peak in the electron density map; (2) the spikes, seen in electron micrographs of negatively stained particles; (3) one or more internal proteins responsible, together with the DNA (which would alone be insufficient), for the continuously high electron density between the centre of the particle and the bilayer. The peak of electron density at a radius about 185 Å (Fig. 4) and the pattern of positive staining in thin section (Fig. 1) suggest that at least some of the internal protein may form a closed shell.

Of the four proteins identified by gel electrophoresis, we can assign component II to the external shell, because it is the species present in largest quantity. A roughly cylindrical subunit of molecular weight 34,000, with a radial extent of 60 Å, will have a diameter of about 30 Å. The broad maximum in the X-ray pattern, centred at 28.5 Å, may therefore indicate the subunit packing in the surface lattice. This interpretation is supported by the observation that the 28.5 Å ring diminishes in intensity with increasing solvent density and vanishes at about 0.40 e/Å^3, as expected for diffraction arising from contrast between protein and intervening solvent spaces. About 800 subunits with an approximately 30 Å packing diameter would cover the particle surface—a number consistent with the estimate of about 650 units/particle based on recovery of radioactively labelled component II in the polyacrylamide gel band.

To account for the shape of the particle and for the positioning of the spikes at the outer vertices, we may assume that at least one component is associated in an icosahedral surface lattice. Possible icosahedral designs for an external shell built of a single protein are T=12 and 13 containing 720 and 780 structure units respectively[26]. If the protein around the five-fold vertices were different from the protein in the faces, the triangulation number of the surface lattice would be larger. We cannot, moreover, rule out a more statistical or liquid-like arrangement for the outer protein, stabilized by an icosahedral internal structure. In either case, the observations from electron microscopy and X-ray diffraction indicate that the outer-shell subunits are not clustered into distinct morphological units such as pentamers and hexamers, which are a prominent feature of some icosahedral viruses[26].

Structure and Assembly

The degree to which the present diffraction experiments specify the molecular organization of the PM2 particle is

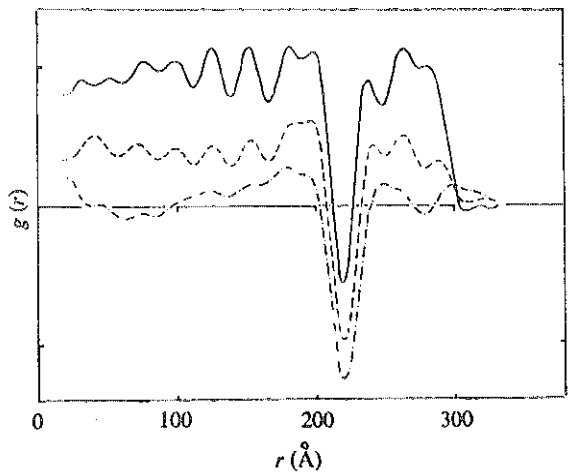

Fig. 4 Fourier syntheses corresponding to the three sets of data shown in Fig. 3. The curves represent the spherically averaged electron density as a function of radius, with the solvent density taken as zero in each case (for solvents, see legend to Fig. 3).

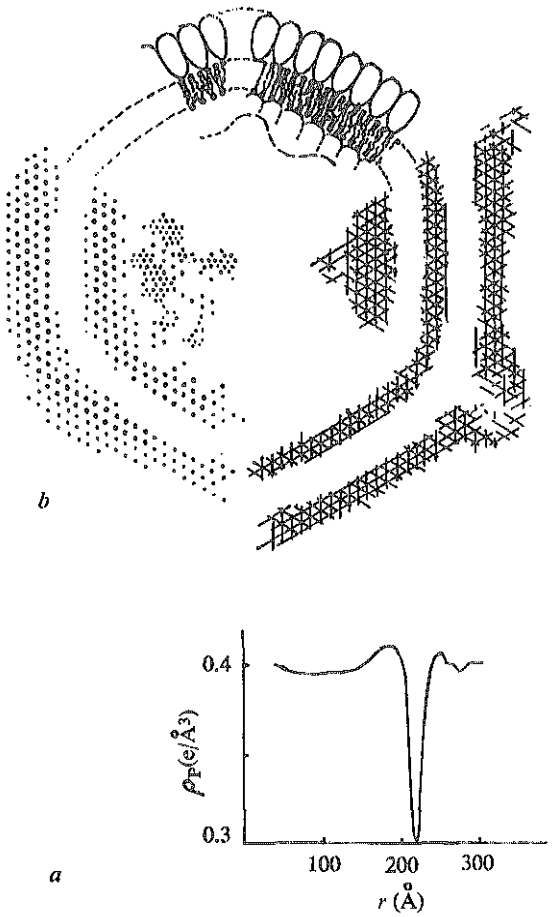

Fig. 5 *a*, Absolute value of the mean electron density of solvent-excluding regions in the PM2 particle, plotted as a function of radius. *b*, Diagram showing relation of the proposed molecular organization in the PM2 particle to images of negatively and positively stained virus. At the top the radial location of principal components is indicated; protein subunits and lipid bilayer are depicted schematically. On the right, the space accessible to negative stain is shown cross-hatched; the upper part corresponds to images in Fig. 1*a*, *b*, labelled B; the lower part, to images labelled A. On the left the positive stain distribution in thin sections is represented by dots. The scale is identical with the abscissa of *a*.

restricted by the resolution and by the spherical averaging. We can summarize interpretation of our results as: (1) lipid is arranged in a bilayer, centred at $r=220$ Å, with an interpolar group distance of about 40 Å; (2) the lipid hydrocarbon chains have a liquid-like packing; (3) the possibility that there is bridging of protein across the bilayer cannot be ruled out, but protein–lipid interactions do not appear to modify the lipid packing significantly; (4) the external protein is probably packed in an icosahedral surface lattice. These features are incorporated into the diagram shown in Fig. 5*b*. The drawing also shows the pattern of negative and positive staining as seen in the electron microscope, in order to indicate interpretation of the observed images in terms of the proposed molecular organization. We note that this arrangement does not conform to conventional structural categories for lipid-containing viruses[27]: "capsid" and "envelope" do not appear clearly distinguished.

We can ask, in view of our picture of the PM2 structure, whether the particle is formed by a process similar to the maturation of enveloped animal viruses[28]. Semliki Forest virus, for example, first assembles a nucleoprotein core, which then acquires its lipid and protein coat by extrusion through the cell membrane[12]. The curvature of the outer surface is apparently stabilized at least in part by the core, which can be isolated separately from infected cells[29]. Cores have also been obtained by breakdown of complete Sindbis particles[30,31]. No internal particle has yet been isolated from PM2, and thin sections of infected cells show no evidence of such a structure. At a sufficiently advanced stage of infection, particles with the appearance of complete PM2 are seen near the inner surface of the cell membrane[32,33]. The micrographs give no evidence for budding. Lysis finally liberates the mature virus. Images that seem to be empty particles, lacking the dense depositions of stain at their centre, appear both in micrographs of some infected cells and in sections of pelleted, purified virus[3,33]. These observations suggest that the formation of the final structure may proceed not by encapsulation of an internal nucleocapsid in an outer envelope but rather by the assembly of protein and lipid around a molecule of DNA. The production of the viral shell presumably involves the biosynthetic mechanisms of cell membrane formation.

We thank Dr J. A. Silbert for the electron micrographs, and Miss Marianne Salditt and Mr Charles Ingersoll jun. for assistance. S. C. H. is a junior fellow in the Society of Fellows, Harvard University. R. D. C.-O. is a New York University School of Medicine predoctoral fellow. This work was supported in part by grants from the National Cancer Institute (to D. L. D. C.) and the National Institute of Allergy and Infectious Diseases (to R. M. F.), US Public Health Service.

Received December 21, 1970.

[1] Espejo, R. T., and Canelo, E. S., *Virology*, **34**, 738 (1968).
[2] Franklin, R. M., Salditt, M., and Silbert, J. A., *Virology*, **38**, 627 (1969).
[3] Silbert, J. A., Salditt, M., and Franklin, R. M., *Virology*, **39**, 666 (1969).
[4] Blaurock, A., *J. Mol. Biol.* (in the press).
[5] Caspar, D. L. D., and Kirschner, D. A., *Nature* (in the press).
[6] Gulik-Krzywicki, T., Rivas, E., and Luzzati, V., *J. Mol. Biol.*, **27**, 303 (1967).
[7] Rand, R. P., and Luzzati, V., *Biophys. J.*, **8**, 125 (1968).
[8] Levine, Y. K., Bailey, A. I., and Wilkins, M. H. F., *Nature*, **220**, 577 (1968).
[9] Gulik-Krzywicki, T., Schechter, E., Luzzati, V., and Faure, M., *Nature*, **223**, 1116 (1969).
[10] Franklin, R. M., *Prog. Med. Virol.*, **4**, 1 (1962).
[11] Klenk, H. D., and Choppin, P. W., *Virology*, **38**, 255 (1969).
[12] Acheson, N. H., and Tamm, I., *Virology*, **32**, 128 (1967).
[13] Simpson, R. W., and Hauser, R. E., *Virology*, **34**, 358 (1968).
[14] Espejo, R., Canelo, E., and Sinsheimer, R. L., *Proc. US Nat. Acad. Sci. (Wash.)*, **63**, 1164 (1969).
[15] Braunstein, S. N., and Franklin, R. M., *Virology* (in the press).
[16] Robertson, J. D., in *Principles of Biomolecular Organization* (edit. by Wostenholme, G. E. W., and O'Connor, M.), 357 (Little, Brown, Boston, 1966).
[17] Harrison, S. C., *J. Mol. Biol.*, **42**, 457 (1969).
[18] Guinier, A., *X-ray Diffraction in Crystals, Imperfect Crystals and Amorphous Bodies* (Freeman, San Franscisco, 1963).
[19] Anderegg, J. W., Geil, P. H., Beeman, W. W., and Kaesberg, P., *Biophys. J.*, **3**, 175 (1963).
[20] Finch, J. T., and Holmes, K. C., in *Methods in Virology* (edit. by Maramorosch, K., and Koprowski, H.), **3**, 351 (Academic Press, New York, 1967).
[21] Wilkins, M. H. F., *Cold Spring Harbor Symp. Quant. Biol.*, **21**, 75 (1956).
[22] Luzzati, V., in *Biological Membranes* (edit. by Chapman, D.), 71 (Academic Press, New York, 1968).
[23] Klug, A., Longley, W., and Leberman, R., *J. Mol. Biol.*, **15**, 315 (1966).
[24] Perutz, M. F., *Trans. Faraday Soc.*, **42** B, 187 (1946).
[25] Chapman, D., in *Biological Membranes* (edit. by Chapman, D.), 125 (Academic Press, New York, 1968).
[26] Caspar, D. L. D., and Klug, A., *Cold Spring Harbor Symp. Quant. Biol.*, **27**, 1 (1962).
[27] Lwoff, A., Horne, R., and Tournier, P., *Cold Spring Harbor Symp. Quant. Biol.*, **27**, 51 (1962).
[28] Morgan, C., Howe, C., and Rose, H. M., *J. Exp. Med.*, **113**, 219 (1961).
[29] Acheson, N. H., and Tamm, I., *Virology*, **41**, 306 (1970).
[30] Strauss, J. H., Burge, B. W., Pfefferkorn, E. R., and Darnell, J. E., *Proc. US Nat. Acad. Sci.*, **50**, 533 (1968).
[31] Horzinek, M., and Mussgay, M., *J. Virol.*, **4**, 514 (1969).
[32] Cota-Robles, E., Espejo, R. J., and Heywood, P. W., *J. Virol.*, **2**, 56 (1968).
[33] Dahlberg, J., and Franklin, R. M., *Virology* (in the press).
[34] Bragg, W. L., and Perutz, M. F., *Proc. Roy. Soc.*, A, **213**, 425 (1952).

Printed in Great Britain by Fisher, Knight & Co., Ltd., St. Albans.